Two-photon spin injection in semiconductors

R. D. R. Bhat, P. Nemec,* Y. Kerachian, H. M. van Driel, and J. E. Sipe
Department of Physics, University of Toronto, 60 St. George Street, Toronto, Ontario, Canada M5S 1A7

Arthur L. Smirl
Laboratory for Photonics & Quantum Electronics, 138 IATL, University of Iowa, Iowa City, Iowa 52242, USA
(Received 12 July 2004; published 18 January 2005)

A comparison is made between the degree of spin polarization of electrons excited by one- and two-photon absorption of circularly polarized light in bulk zinc-blende semiconductors. Time- and polarization-resolved experiments in (001)-oriented GaAs reveal an initial degree of spin polarization of 49% for both one- and two-photon spin injection at wavelengths of 775 and 1550 nm, in agreement with theory. The macroscopic symmetry and microscopic theory for two-photon spin injection are reviewed, and the latter is generalized to account for spin-splitting of the bands. The degree of spin polarization of one- and two-photon optical orientation need not be equal, as shown by calculations of spectra for GaAs, InP, GaSb, InSb, and ZnSe using a 14×14 $\mathbf{k}\cdot\mathbf{p}$ Hamiltonian including remote band effects. By including the higher conduction bands in the calculation, cubic anisotropy and the role of allowed-allowed transitions can be investigated. The allowed-allowed transitions do not conserve angular momentum and can cause a high degree of spin polarization close to the band edge; a value of 78% is calculated in GaSb, but by varying the material parameters it could be as high as 100%. The selection rules for spin injection from allowed-allowed transitions are presented, and interband spin-orbit coupling is found to play an important role.

DOI: 10.1103/PhysRevB.71.035209 PACS number(s): 72.25.Fe, 42.65.−k, 78.47.+p, 72.25.Rb

I. INTRODUCTION

The optical injection of spin-polarized electrons in semiconductors, familiar since the 1980s,[1] is again attracting attention, due in part to the potential utilization of a spin-polarized electrical current in a technology called "spintronics."[2,3] It is well known that linear absorption of circularly polarized light in a semiconductor produces spin-polarized electrons in the conduction band.[1] This occurs as a result of the entanglement of electron spin and motion caused by the spin-orbit coupling in the material; in the absence of spin-orbit coupling, there would be no net spin polarization of the excited carriers. For many common semiconductors, the highest valence states are in the degenerate heavy and light hole bands at the Γ point. Consequently, the highest degree of spin polarization that can be achieved is 50%. Such a situation occurs when the photon energy exceeds the band gap, but is not large enough to excite carriers out of the split-off band. This can be understood from selection rules that result from the symmetry of the states at the Γ point.[1]

One way to increase the spin polarization of the injected electrons is to use materials where the degeneracy between heavy and light hole bands is removed by strain and/or quantum confinement, so that one can excite carriers only from one band. From the symmetry of the states, one then expects 100% spin polarization. And indeed both theory[1] and experiments[4,5] have shown a significant enhancement of the degree of spin polarization. The spin polarization could also be increased by using compounds with crystal structures having no valence band degeneracy.[6–8]

Spin injection can also arise from two-photon absorption. For certain applications this may have advantages over one-photon spin injection due to a much longer absorption depth, which allows spin excitation throughout the volume of a bulk sample. Two-photon spin injection has been investigated in lead chacogenides (PbTe, PbSe, and PbS), which are cubic, and have direct fundamental band gaps at the L points.[9] High degrees of spin polarization in these materials have been predicted,[9] but not observed.[10–13] Our focus in this paper is on semiconductors that have a direct fundamental band gap at the Γ point, such as GaAs. Based on arguments involving the conservation of angular momentum, it was recently suggested that 100% spin polarization could be achieved in unstrained bulk GaAs from two-photon absorption.[14] Earlier theoretical calculations, however, predict a two-photon spin polarization of no more than 64% for this class of cubic semiconductors.[9,15–17]

In this paper, we report results of time-resolved pump-probe experiments that show the degrees of spin polarization from one- or two-photon absorption are in fact comparable for GaAs. We also discuss in detail the various effects that can complicate the direct experimental comparison of the spin polarization obtained by one- and two-photon excitation. We present microscopic calculations of two-photon spin injection that go beyond the spherical approximation made by earlier calculations. We show how the simple argument based on conservation of angular momentum breaks down, and examine the transitions that give rise to the partial spin polarization. The calculated one- and two-photon degrees of spin polarization are not equal for all materials, and we find that, in fact, two-photon spin injection can be fully polarized, but only from transitions that do *not* conserve angular momentum.

Optical transitions near the Γ point can be summarized with sketches such as those in Fig. 1. The symmetry of the states at the Γ point of a crystal with zinc-blende symmetry is as follows. The conduction band (Γ_{6c}) is s-like with two

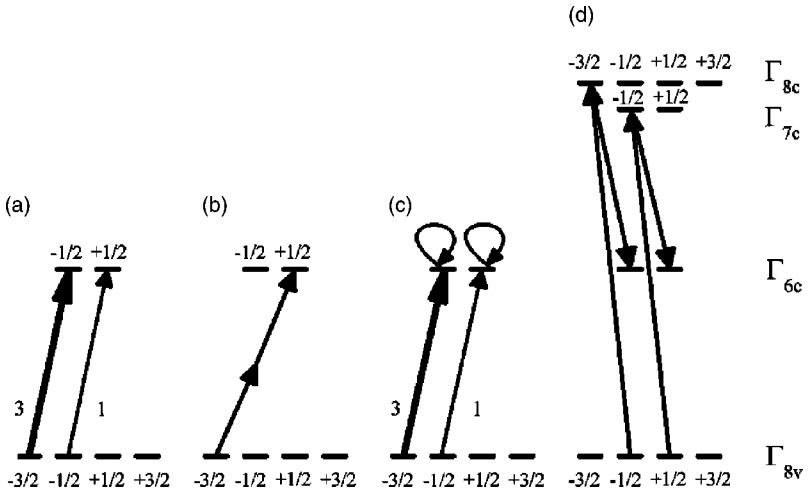

FIG. 1. Optical transitions in a bulk zinc-blende semiconductor for circularly polarized light σ^+ allowed by the selection rules: (a) for one-photon absorption, (b) for two-photon absorption as suggested by Matsuyama *et al.* (Ref. 14), (c) two-photon allowed-forbidden transitions with a conduction band as an example of an intermediate state, and (d) two-photon allowed-allowed transitions for vanishing interband spin-orbit coupling and light incident along a $\langle 001 \rangle$ direction. The quantum number m_j for the projection of total angular momentum on the light propagation direction of all states involved is indicated in the figures. The thickness of arrows and adjacent number in (a) and (c) express the relative transition probabilities.

degenerate spin states, while the valence bands are *p*-like. The *p*-like orbitals are coupled to the electron spin to form four states (the heavy and light hole bands, Γ_{8v}) that are total angular momentum ($j=3/2$)-like, and two states at lower energy (the split-off band, Γ_{7v}) that are ($j=1/2$)-like.[18] Note that these states are commonly referred to as if they were eigenstates of total angular momentum, even though they are not.[18] The levels corresponding to the split-off band are not shown in Fig. 1. The selection rules for the transitions between these states are the same as for the states of a spherically symmetric system.[1] Thus they can be understood using angular momentum arguments. By applying the familiar selection rule that one-photon absorption of circularly polarized light with positive helicity (σ^+) must change the projection of total angular momentum by $+1$, one sees that only the two transitions shown in Fig. 1(a) are allowed. An examination of Clebsch-Gordan coefficients reveals that the transition from the $m_j=-3/2$ state of the valence band to the $m_j=-1/2$ state of the conduction band is three times as probable as the transition from the $m_j=-1/2$ state of the valence band to the $m_j=+1/2$ of the conduction band. Thus, near the band edge, one expects a value of 50% for the degree of electron spin polarization

$$P \equiv \frac{N_\downarrow - N_\uparrow}{N_\downarrow + N_\uparrow}, \tag{1}$$

where $N_\downarrow$ ($N_\uparrow$) is the concentration of electrons with spin down (up).

The idea of angular momentum conservation was applied to two-photon absorption by Matsuyama *et al.*[14] They argue that because the total angular momentum of the two right circularly polarized photons is $+2$, only the transition from $m_j=-3/2$ to $m_j=+1/2$ is allowed [see also Fig. 1(b)]. Therefore they suggest that even in a bulk semiconductor with degenerate valence bands the resulting electron spin polarization should be 100%, and indeed with an opposite sign with respect to one-photon spin injection.

On the other hand, the degree of spin polarization due to two-photon spin injection has been calculated several times[9,15–17] using the eight band Kane model.[19] Ivchenko calculated the degree of spin polarization in the limit of large spin-orbit splitting.[9,15] Arifzhanov and Ivchenko improved the calculation by allowing the split-off band to act as an intermediate state; they gave the degree of spin polarization at the band edge as a function of E_g/Δ, where E_g is the band gap energy and Δ is the spin-orbit splitting.[16] For GaAs, one infers a 51% degree of spin polarization from their results. Note that, in contrast to one-photon spin injection, the degree of spin polarization of two-photon spin injection near the band edge depends not only on the symmetry of the states, but also on various material parameters. When only two-band transitions are included, a very simple expression for the two-photon degree of spin polarization has been given in terms of the conduction and valence band effective masses,[17] from which one infers for GaAs a spin polarization of 48%.

In most III-V semiconductors, the next higher conduction bands are *p*-like (Γ_{7c} and Γ_{8c}).[18] The role that these higher bands play in two-photon spin injection has not previously been investigated. It is known that $\mathbf{k}\cdot\mathbf{p}$ mixing with these bands is responsible for cubic anisotropy of two-photon absorption.[20,21] The higher conduction bands can also act as intermediate states in the two-photon amplitude. Such transitions are qualitatively different than transitions within the set of bands nearest to the fundamental band gap.[22–25]

In Sec. II we review the symmetry of two-photon spin injection and present our calculation including the higher conduction bands. In contrast to previous calculations of two-photon spin injection,[9,15–17] our calculation is not perturbative in *k*. In Sec. III we present the experimental comparison of one- and two-photon spin injection. In Sec. IV we discuss the transitions responsible for the degree of spin polarization in two-photon absorption [Figs. 1(c) and 1(d)]. In Appendix B we derive expressions for the degree of two-photon spin injection due to so-called "allowed-allowed" transitions.

II. CALCULATION OF TWO-PHOTON SPIN INJECTION

For an electric field of the form $\mathbf{E}(t)=\mathbf{E}_\omega \exp(-i\omega t)+\text{c.c.}$ (we sometimes write $\mathbf{E}_\omega = E_\omega \hat{\mathbf{e}}_\omega$), the two-photon spin injection rate can be written phenomenologically as $\dot{S}^i = \zeta^{ijklm} E^j_\omega E^k_\omega E^{l*}_\omega E^{m*}_\omega$, where ζ^{ijklm} is a fifth rank pseudotensor

symmetric on exchange of indices j and k, and on exchange of indices l and m; superscript lowercase letters denote Cartesian components and repeated indices are to be summed over.[26] For the point groups T_d and O_h, appropriate to most cubic semiconductors, a general fifth rank pseudotensor has ten independent components. Forcing the $j \leftrightarrow k$ and $l \leftrightarrow m$ symmetries, and the condition for reality of $\dot{\mathbf{S}}$, $\zeta^{ilmjk} = (\zeta^{ijklm})^*$, leaves three independent real components.

We define $\zeta_{2A} \equiv -i\zeta^{abccc}$ and $\zeta_{2B} \equiv \mathrm{Im}\,\zeta^{aabac}$, where the indices a, b, and c denote components along the standard cubic axes [100], [010], and [001]. Then the three independent real components are Re ζ_{2A}, Im ζ_{2A}, and ζ_{2B}. In the standard cubic basis, the nonzero components of ζ are

$$\zeta^{abbbc} = \zeta^{abccc} = \zeta^{bacaa} = i\zeta_{2A};$$

$$\zeta^{bccac} = \zeta^{caaab} = \zeta^{cabbb} = i\zeta_{2A};$$

$$\zeta^{abcbb} = \zeta^{accbc} = \zeta^{baaac} = -i\zeta_{2A}^{*};$$

$$\zeta^{baccc} = \zeta^{cabaa} = \zeta^{cbbab} = -i\zeta_{2A}^{*};$$

$$\zeta^{aabac} = \zeta^{bbcab} = \zeta^{cacbc} = i\zeta_{2B};$$

$$\zeta^{aacab} = \zeta^{babbc} = \zeta^{cbcac} = -i\zeta_{2B},$$

as well as those generated by exchanging $j \leftrightarrow k$ and/or $l \leftrightarrow m$, for a total of 48 components.

The point group symmetry allows spin injection for linearly polarized light, associated with Imζ_{2A}. However, from a microscopic expression for ζ in the independent particle picture [see Eqs. (4), (6), and (7) below], one can show that ζ must be purely imaginary due to the time reversal properties of the Bloch states. One might expect deviations from the independent particle picture within an exciton binding energy of the band edge.[24,27] In what follows, we assume the independent particle picture is valid, which leaves the two-photon spin injection specified in terms of two real parameters ζ_{2A} and ζ_{2B}.

The component of the spin injection rate along one of the cubic axes can be written compactly (with no summation convention) as[9]

$$\dot{S}^i = 2i(\mathbf{E}_\omega \times \mathbf{E}_\omega^*)^i \left[\zeta_{2A}|\mathbf{E}_\omega|^2 + (2\zeta_{2B} - \zeta_{2A})|E_\omega^i|^2\right]. \quad (2)$$

If the material were isotropic, the spin injection rate could be described by only one real parameter; $\zeta_{2A} = 2\zeta_{2B}$ and the second term in Eq. (2) would be zero.

The cubic anisotropy means that the two-photon spin injection from circularly polarized light depends on the angle of incidence of the light relative to the cubic axes. For circularly polarized light incident along $\hat{\mathbf{n}}$ specified by polar angles θ and ϕ relative to the cubic axes,

$$\dot{\mathbf{S}} \cdot \hat{\mathbf{n}} = \mp 2\zeta_{2A}|E_\omega|^4 \left(1 + \frac{2\zeta_{2B} - \zeta_{2A}}{4\zeta_{2A}} f(\theta, \phi)\right), \quad (3)$$

where $f(\theta, \phi) = \sin^2(2\theta) + \sin^4(\theta)\sin^2(2\phi)$. The upper (lower) sign is for right (left) circular polarization. The analogous equation for two-photon absorption is given by Hutchings and Wherrett[21]. Equation (3) has extrema for light incident along $\langle 001 \rangle$ and $\langle 111 \rangle$ directions. Due to the cubic anisotropy, the net injected spin is not always parallel to $\hat{\mathbf{n}}$, although it is when $\hat{\mathbf{n}}$ is along $\langle 001 \rangle$ or $\langle 111 \rangle$. In particular, for light along a $\langle 001 \rangle$ direction, $|\dot{\mathbf{S}}| = 2\zeta_{2A}|E_\omega|^4$, while for light incident along a $\langle 111 \rangle$ direction, $|\dot{\mathbf{S}}| = (4/3)(\zeta_{2A} + \zeta_{2B})|E_\omega|^4$.

A. Microscopic calculation

We calculate the photoinjection rate of net electron spin density, $\dot{\mathbf{S}}$, using second order perturbation theory with the light treated classically in the long wavelength limit. We ignore interactions amongst the electrons, and between electrons and phonons. We take the photon energy to be below the band gap, and twice the photon energy to be above the band gap. We neglect any spin polarization of the holes, since their spin relaxation times are typically very short.[28] In the Fermi's golden rule (FGR) limit, the photoinjection rate is time-independent.

Expressions for the two-photon spin injection rate under these assumptions have been given before.[9,16,17,26] However, all previous calculations used semiconductor models in which all bands are doubly degenerate. In such a case, one finds that

$$\dot{\mathbf{S}} = \frac{2\pi}{L^3} \sum_{c,c',v,\mathbf{k}}{}' \langle c\mathbf{k}|\hat{\mathbf{S}}|c'\mathbf{k}\rangle \Omega^{(2)*}_{c,v,\mathbf{k}} \Omega^{(2)}_{c',v,\mathbf{k}} \delta[2\omega - \omega_{cv}(\mathbf{k})], \quad (4)$$

where $|n\mathbf{k}\rangle$ is a Bloch state with energy $\hbar\omega_n(\mathbf{k})$, L^3 is a normalization volume, $\hat{\mathbf{S}}$ is the spin operator, $\omega_{nm}(\mathrm{k}) \equiv \omega_n(\mathbf{k}) - \omega_m(\mathbf{k})$, the prime on the summation indicates a restriction to pairs (c, c') for which $\omega_{cc'} = 0$, and $\Omega^{(2)}_{c,v,\mathbf{k}}$ is the two-photon amplitude

$$\Omega^{(2)}_{c,v,\mathbf{k}} = \left(\frac{e}{\hbar\omega}\right)^2 \sum_n \frac{[\mathbf{E}_\omega \cdot \mathbf{v}_{c,n}(\mathbf{k})][\mathbf{E}_\omega \cdot \mathbf{v}_{n,v}(\mathbf{k})]}{\omega_{nv} - \omega(\mathbf{k})}, \quad (5)$$

with $\mathbf{v}_{n,m}(\mathbf{k}) \equiv \langle n\mathbf{k}|\hat{\mathbf{v}}|m\mathbf{k}\rangle$, where $\hat{\mathbf{v}}$ is the velocity operator. It is well known, however, that in real crystals of zinc-blende symmetry the spin degeneracy is removed,[29,30] albeit with a small energy splitting. Since we are using a model that accounts for this spin-splitting,[31] we must generalize the earlier microscopic expressions. Such a generalization was recently discussed for one-photon spin injection.[32]

If the spin-split bands are well separated, FGR gives

$$\dot{\mathbf{S}} = \frac{2\pi}{L^3} \sum_{c,v,\mathbf{k}} \langle c\mathbf{k}|\hat{\mathbf{S}}|c\mathbf{k}\rangle |\Omega^{(2)}_{c,v,\mathbf{k}}|^2 \delta[2\omega - \omega_{cv}(\mathbf{k})]. \quad (6)$$

However, in GaAs the splitting is at most a few meV for conduction states within 500 meV of the band edge.[33] Since this is comparable to the broadening that one would calculate from the scattering time of the states (and also to the laser bandwidth for experiments with pulses shorter than 100 fs), spin-split pairs of bands should be treated as quasidegenerate in FGR. Thus in place of Eq. (4) and (6) we use

TABLE I. Model parameters.

	GaAs	InP	GaSb	InSb	ZnSe
E_g (eV)	1.519	1.424	0.813	0.235	2.820
Δ_0 (eV)	0.341	0.108	0.75	0.803	0.403
E_0' (eV)	4.488	4.6	3.3	3.39	7.330
Δ_0' (eV)	0.171	0.50	0.33	0.39	0.090
Δ^- (eV)	−0.061	0.22	−0.28	−0.244	−0.238
P_0 (eV Å)	10.30	8.65	9.50	9.51	10.628
Q (eV Å)	7.70	7.24	8.12	8.22	9.845
P_0' (eV Å)	3.00	4.30	3.33	3.17	9.165
γ_{1L}	7.797	5.05	13.2	40.1	4.30
γ_{2L}	2.458	1.6	4.4	18.1	1.14
γ_{3L}	3.299	1.73	5.7	19.2	1.84
F	−1.055	0	0	0	0
C_k (meV Å)	−3.4	−14	0.43	−9.2	−14

$$\dot{\mathbf{S}} = \frac{2\pi}{L^3} \sum_{c,c',v,\mathbf{k}}' \langle c\mathbf{k}|\hat{\mathbf{S}}|c'\mathbf{k}\rangle \Omega^{(2)*}_{c,v,\mathbf{k}} \Omega^{(2)}_{c',v,\mathbf{k}} \times \frac{1}{2}\{\delta[2\omega - \omega_{cv}(\mathbf{k})] + \delta[2\omega - \omega_{c'v}(\mathbf{k})]\}, \tag{7}$$

where the prime on the summation indicates a restriction to pairs (c,c') for which either $c'=c$, or c and c' are a quasidegenerate pair. The coherence between quasidegenerate bands is optically excited and grows with their populations, as is the case with simpler band models that neglect spin splitting.[9,15–17,26] Using the time reversal properties of the Bloch functions, the expression for ζ^{ijklm} that follows from Eq. (7) can be simplified to give

$$\zeta^{ijklm} = i\left(\frac{e}{\hbar\omega}\right)^4 \frac{2\pi}{L^3} \sum_{c,c',v,\mathbf{k}}' \sum_{n,n'} \delta[2\omega - \omega_{cv}(\mathbf{k})] \times \mathrm{Im}\left[\frac{\langle c\mathbf{k}|\hat{S}^i|c'\mathbf{k}\rangle (V^{jklm} - V^{lmjk})/2}{[\omega_{nv}(\mathbf{k}) - \omega][\omega_{n'v}(\mathbf{k}) - \omega]}\right], \tag{8}$$

where

$$\mathbf{V}^{jklm} \equiv \{\mathbf{v}_{c',n'}(\mathbf{k}), \mathbf{v}_{n',v}(\mathbf{k})\}^{jk} \{\mathbf{v}^*_{c,n}(\mathbf{k}), \mathbf{v}^*_{n,v}(\mathbf{k})\}^{lm},$$

and $\{\mathbf{v}_1,\mathbf{v}_2\}^{ij} \equiv (v_1^i v_2^j + v_1^j v_2^i)/2$.

The photoinjection rate for the density of electron-hole pairs is

$$\dot{N} = \frac{2\pi}{L^3} \sum_{c,v,k} |\Omega^{(2)}_{c,v,\mathbf{k}}|^2 \delta[2\omega - \omega_{cv}(\mathbf{k})]. \tag{9}$$

From Eqs. (7) and (9), the degree of spin polarization, P, can be calculated, since

$$P = -\frac{2}{\hbar}\frac{\dot{\mathbf{S}}\cdot\hat{\mathbf{n}}}{\dot{N}}. \tag{10}$$

The sign of P is chosen so that a positive P corresponds to an excess of electrons with spin down, i.e., spin opposite the photon angular momentum.

To evaluate the degree of spin polarization, we use a $\mathbf{k}\cdot\mathbf{p}$ model that diagonalizes the one-electron Hamiltonian (including spin-orbit coupling) within a basis set of 14 Γ point states, and includes important remote band effects.[31] Fourteen band models (also called five-level models) have been used to calculate bandstructures,[34–37] as well as linear[32,38] and nonlinear[21,39,40] optical properties of GaAs and other semiconductors. Winkler has given a recent review of 14 band models.[41] The 14 states (counting one for each spin) comprise six valence band states (the split-off, heavy, and light hole bands), and eight conduction band states (the two lowest, which are *s*-like, and the six next-lowest, which are *p*-like). The states are given in more detail in Appendix A, and except for the split-off hole states, they are shown in Fig. 1(d).

The model contains 13 parameters chosen to fit low-temperature experimental data. Of the two parameter sets discussed by Pfeffer and Zawadzki for GaAs, we use the one corresponding to $\alpha=0.085$ that they find gives better results.[31] For InP, GaSb, and InSb, we use parameters from Cardona, Christensen, and Fasal.[33] The parameters are listed in Table I and the notation is described in Appendix A. For cubic ZnSe, we use the parameters given by Mayer and Rossler[37] and a calculated value of C_k;[33] we use $\Delta^- = -0.238$ eV to give a k^3 conduction band spin-splitting that matches the *ab initio* calculation of Cardona, Christensen, and Fasal.[33] There is more uncertainty in the parameters for ZnSe than in those for the other materials,[37] but we include it as an example of a semiconductor with a larger band gap.

Note that although remote band terms are included in the 14×14 Hamiltonian, we have neglected the remote band contributions to the velocity operator. The effect of these

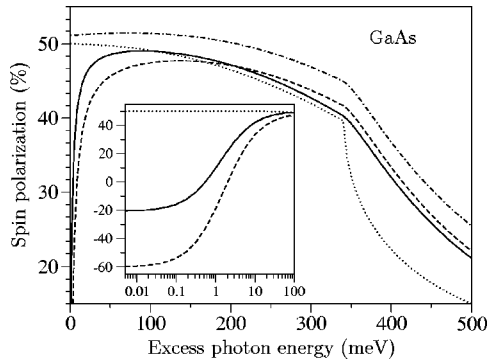

FIG. 2. Calculated degree of electron spin polarization P in GaAs. The solid (dashed) line is for two-photon excitation with light incident along a $\langle 001\rangle$ ($\langle 111\rangle$) direction and the dotted line is for one-photon excitation. The dash-dotted line is for two-photon excitation calculated with an eight band (Γ_{7v}, Γ_{8v}, and Γ_{6c}) spherical model. The inset shows P close to the band edge. The sign of P is given by Eq. (10).

contributions on one-photon absorption was discussed by Enders *et al.*[42] Removing the remote band terms from our Hamiltonian changes P for GaAs by at most 2%. Thus we feel justified in our neglect of the remote band contributions to the velocity operator. Another contribution to the velocity operator $\hat{\mathbf{v}}$, the anomalous velocity term, $\hbar(\boldsymbol{\sigma}\times\boldsymbol{\nabla}V)/(4m^2c^2)$ should be included if k-dependent spin-orbit coupling is included in the 14×14 Hamiltonian. For the results reported in the following section, we have neglected k-dependent spin-orbit coupling. To test whether this neglect is justified, we have repeated the calculation for GaAs including such coupling only between valence and lowest conduction bands and the associated anomalous velocity; the coupling is parametrized by $C_0=0.16$ eV Å (Ref. 43) (note that C_0 is distinct from the k-linear term C_k). It decreases the two-photon P by $\approx 2\%$ for excess energies between 0.1 and 200 meV. The decrease increases for larger excess energy, reaching $\approx 5\%$ for an excess energy of 500 meV.

Our two-photon spin injection calculation is similar to the two-photon absorption calculation of Hutchings and Wherrett.[21] We can reproduce their results by removing remote band effects, which they did not include.

B. Calculation results

The calculated degrees of electron spin polarization, P, are shown for GaAs, InP, GaSb, InSb, and cubic ZnSe in Figs. 2–4 as a function of excess photon energy, $2\hbar\omega - E_g$, where E_g is the fundamental band gap. We also show, for comparison, the degree of electron spin polarization due to one-photon absorption.[32] For each semiconductor, the one-photon degree of spin polarization is 50% at the band edge as expected from the Γ point selection rules.

In GaAs, so long as the excess photon energy is less than the split-off energy (341 meV) and greater than about 50 meV, there is a near equality of one- and two-photon P's.

Close to the band edge, however, there is a feature of the two-photon P that has not previously been identified; it is seen more clearly in the insets of Figs. 2–4. The values of the two-photon P at the band edge for each material are listed in Table II. We discuss this feature further in Sec. IV, but we note here that it does not appear in a spherical approximation. To show this, we have calculated the two-photon P with the 8×8 Kane model that includes only the valence bands and the Γ_{6c} conduction bands, has $C_k=0$, and has γ_2 and γ_3

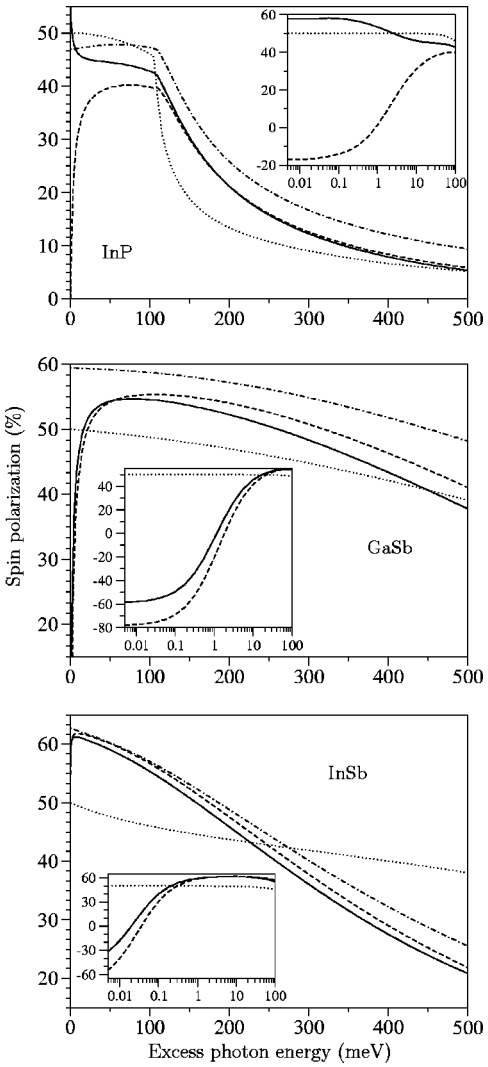

FIG. 3. Same as Fig. 2, but for InP, GaSb, and InSb.

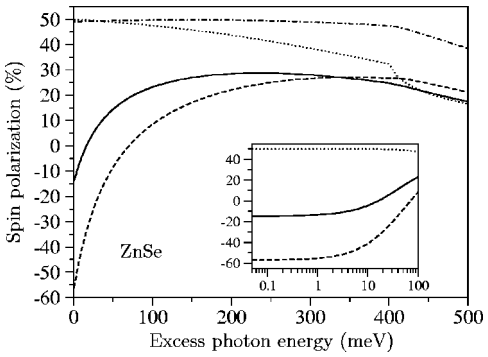

FIG. 4. Same as Fig. 2, but for cubic ZnSe.

TABLE II. Calculated band-edge two-photon P.

	GaAs (%)	InP (%)	GaSb (%)	InSb (%)	ZnSe (%)
[001]	−20.5	58.7	−58.9	−49.3	−14.5
[111]	−60.0	−16.6	−78.4	−73.3	−57.1

replaced by $\tilde{\gamma} \equiv (2\gamma_2 + 3\gamma_3)/5$ to give spherical bands;[44] the result, which is independent of crystal orientation, is shown in the dash-dotted line in Figs. 2–4.

Both one- and two-photon P's decrease as the excess photon energy is increased. This is due to band mixing away from the Γ point, which changes the selection rules. At excess photon energies above the split-off energy, the one-photon P decreases due to transitions from the split-off valence band.[1] The two-photon P also decreases due to these transitions, but less so.

The possibility of cubic anisotropy in two-photon spin injection was first pointed out by Ivchenko,[9] although it has not been calculated until now. Cubic anisotropy in two-photon absorption, on the other hand, has been calculated by Hutchings and Wherrett.[21] They found that near the band edge two-photon absorption of circularly polarized light in GaAs should be about 10% greater for light incident along [111] compared to along [001].[21] The results of our calculation for GaAs indicate that two-photon spin injection varies with crystal orientation by a similar amount. Hence the degree of spin polarization shown in Fig. 2, which is the ratio of the two, varies with crystal orientation by only a few percent for most photon energies in the range we investigated. This is not the case, however, for excess photon energies very close to the band gap, as can be seen in the inset of Fig. 2. The cubic anisotropy is more substantial for ZnSe and InP.

III. EXPERIMENTAL COMPARISON

To experimentally measure the degree of electron spin polarization we performed a polarization-resolved pump-probe experiment, where the transmission of the probe pulses is measured as a function of the delay between ≈150 fs circularly polarized pump and probe pulses. Specifically, we measure the differential transmission $\Delta T/T = (T_E - T_0)/T_0$, where $T_E(T_0)$ is the transmission with (without) the pump. If the absorbance change induced by the pump is small (i.e., $\Delta\alpha l \ll 1$, where l is the sample thickness and $\Delta\alpha = \alpha_E - \alpha_0$ is the difference between the absorption coefficient with and without the pump, respectively), the differential transmission will be proportional to $-\Delta\alpha l$. Furthermore, if this weak absorption change is caused by phase-space filling associated with a thermalized nondegenerate distribution of carriers, then the differential transmission will be proportional to the carrier density ($\Delta T/T \propto N$). These conditions are usually satisfied after about 0.5 ps for thin samples, low carrier densities, and relatively high temperatures. Finally, if the holes do not contribute significantly to the phase-space filling, then the degree of polarization can be experimentally determined by measuring the differential transmission for pump and probe pulses having the same $(\Delta T/T)^{++}$ and opposite $(\Delta T/T)^{+-}$ circular polarizations. For probe pulses near the band edge, $(\Delta T/T)^{++} \propto 3N_{\downarrow} + N_{\uparrow}$ and $(\Delta T/T)^{+-} \propto 3N_{\uparrow} + N_{\downarrow}$, as a result of the same selection rules described above in Sec. I. Defining,

$$P_{\mathrm{exp}} \equiv 2\frac{(\Delta T/T)^{++} - (\Delta T/T)^{+-}}{(\Delta T/T)^{++} + (\Delta T/T)^{+-}}, \tag{11}$$

we then have $P_{\mathrm{exp}} = P$. However, if these restricted conditions are not met, then P_{exp} may not directly yield the degree of polarization. The degree of polarization and the spin relaxation time may still be extracted, but other effects may have to be considered.[45]

Polarization-resolved differential transmission measurements were performed using pulses from an optical parametric amplifier (OPA)[46] pumped by a regeneratively amplified Ti:sapphire laser operating at 250 kHz. The laser system was tuned to produce ≈150 fs pulses at 1550 nm (signal) and 1650 nm (idler). Two beta barium borate (BBO) crystals were used to generate 775 nm pulses from the signal beam and 825 nm pulses from the idler beam. The second-harmonic and fundamental pulses were then separated using dichroic beamsplitters. Thus we used 775 nm pulses to excite the sample by one-photon absorption, 1550 nm pulses to excite the sample by two-photon absorption, and 825 nm pulses to probe the transmission of the sample.

We used a semi-insulating (impurity level less than 10^{15} cm^{-3}), 1 μm thick sample of [001]-grown bulk GaAs that was van der Waals bonded to the glass substrate. The experiments were performed at a temperature of 80 K. Consequently, the probe beam was resonant with the band gap energy E_g, and the pump beams had an excess energy $(2\hbar\omega - E_g)$ of 90 meV, which is considerably less than the spin-orbit splitting energy of 341 meV. The peak irradiances of pump pulses were ≈2.3 GW/cm^2 (fluence ≈320 μJ/cm^2) for two-photon and ≈11 MW/cm^2 (fluence ≈1.2 μJ/cm^2) for one-photon absorption, exciting in both cases a carrier density of $\approx 6 \times 10^{16}$ cm^{-3}. Probe pulses were 10 times weaker than pump pulses for one-photon excitation.

The design and implementation of the experiments involved a substantial effort to remove all possible experimental artifacts that could influence direct comparison of the results obtained for optical pumping by one- and two-photon absorption. First, by using a pump-probe technique, we directly measured the degree of spin polarization of electrons at fixed times after the generation process. Thus our data are more credible than that of experiments using time-integrated methods, where the measured degree of spin polarization has to be corrected using the ratio of the lifetime and the spin relaxation time of electrons.[14,15] Second, we used a relatively thin layer of GaAs. One- and two-photon absorption have substantially different excitation depth profiles, the former being considerably steeper than the latter. In order to directly use Eq. (11) to determine the degree of spin polarization, it is necessary to keep the sample thin enough to ensure that $\Delta\alpha l \ll 1$ for each process; however, the sample must be kept as thick as possible to maximize the magnitude of $\Delta T/T$. We selected a 1 μm thickness as a compromise between these

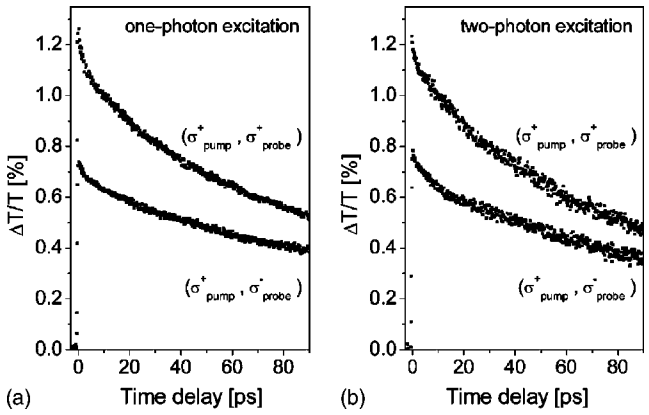

FIG. 5. The dynamics of differential transmission $\Delta T/T$ after excitation by circularly polarized pump pulses with the excess energy of 90 meV as measured using probe pulses with the same (upper curve) and opposite (lower curve) circular polarization for one-photon (a) and two-photon (b) excitation.

two tendencies. For the sample temperature and the wavelengths used here, the transmissions T of pump pulses for the two-photon excitation were larger than 99%. For pump pulses for one-photon excitation $T \approx 30\%$, and for the probe pulses $T \approx 70\%$.[47] Third, by using a probe wavelength different from the pump, we were able to improve the signal-to-noise ratio by using a spectral filter to eliminate scattered pump light. Fourth, we precisely characterized the quality of the circular polarization of all optical beams used. Due to the finite spectral bandwidth of the femtosecond optical pulses and the quality of the quarter wave $(\lambda/4)$ plates, the optical beams were not 100% circularly polarized, but instead consisted of both σ^+ and σ^-. However, the quality of the circular polarization of both pumps beams was nearly the same. A nominal σ^+ polarization state of pump pulses for one-photon excitation was 95% σ^+ and 5% σ^-, while for two-photon excitation a nominal σ^+ polarization state was 94% σ^+ and 6% σ^-. As another check, we used a broadband quarter wave plate to monitor the helicity of all beams. Finally, to avoid problems due to possible sample inhomogeneity, we focused all three beams (the pump beams for one- and two-photon excitation, and the probe beam) to the same position on the sample using a single achromatic lens. Their mutual spatial overlap was checked using a pinhole.

The results of the pump-probe experiment for one-photon excitation by a σ^+ pump are shown in Fig. 5(a). The upper curve corresponds to probing with a σ^+ probe, while the lower curve was measured with a σ^- probe. The difference between the different polarization conditions is caused by spin-dependent phase-space filling as described above. The resulting electron spin polarization P as a function of time delay is Fig. 6 (closed squares). The decay of P is due to the randomization of the initial spin polarization. From the data depicted in Fig. 6 we infer a time constant of ≈ 200 ps, which is conventionally considered as half of the spin relaxation time. The dominant spin relaxation mechanism is probably the precession about anisotropic internal magnetic fields (the D'yakonov-Perel' mechanism).[48–50] For two-photon excitation by a σ^+ pump, the $\Delta T/T$ signal was the same as in the case of one-photon excitation as illustrated in Fig. 5(b).

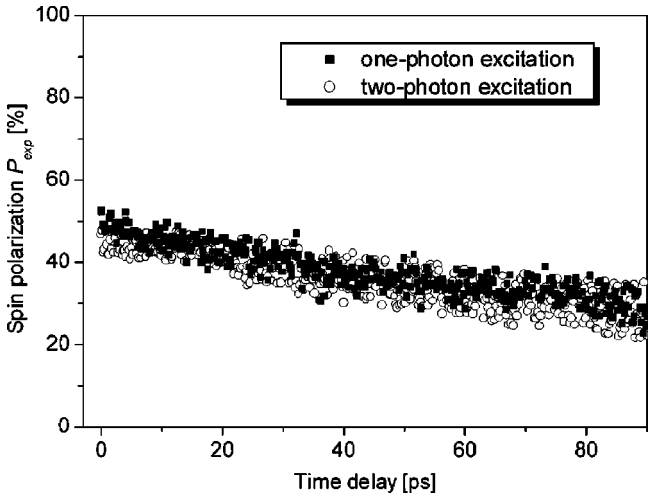

FIG. 6. The dynamics of the degree of spin polarization of electrons P_{exp} after one-photon (closed squares) and two-photon (open circles) excitation as computed from data shown in Fig. 5.

The resulting values of spin polarization P are shown in Fig. 6 (open circles) as a function of time delay. We can now directly compare the results obtained for one- and two-photon excitation. First, note that after excitation by σ^+ pump pulses P has the *same sign* in both cases, in a clear contrast to the predictions made by Matsuyama *et al.*[14] [see Fig. 1(b)]. Second, the initial values of P for both one- and two-photon excitations are, within the experimental error (including the nonideal polarization state of optical pulses used), the same and equal to the theoretical value of 49% expected for both at these photon energies.

IV. DISCUSSION

The prediction of a 100% degree of two-photon spin injection mentioned in Sec. I uses arguments familiar from spherically symmetric systems. At first it might seem incorrect to even apply these in cubic systems, for the crystal Hamiltonian is not rotationally invariant and thus does not conserve angular momentum: The lattice is viewed as fixed and able to provide any amount of torque. However, the deviation from spherical symmetry is small in many cases, and hence angular momentum arguments should have approximate validity. Stated more technically, since T_d is a subgroup of O_h, which is a subgroup of the full rotation group, the Hamiltonian can be written as the sum of spherical, cubic, and tetrahedral parts with the latter two treated as perturbations.[41,44,51–53] The eight band Kane model (even including remote band effects but with $\gamma_{2L}=\gamma_{3L}$ and $C_k=0$) is spherically symmetric and is often used to describe many properties. It has been used, in particular, for earlier calculations of one- and two-photon spin injection.[1,9,15–17] In a spherical model, however, the transitions depicted in Fig. 1(b) do not occur. By examining the possible intermediate states [i.e., band n in Eq. (5)], we can see which transitions do occur, and understand the transfer of angular momentum.

A. Allowed-forbidden transitions

When the intermediate state is in the same band as either the initial or final state (a so-called "two-band transition"),

one of the photons causes an intraband transition. These two-band transitions dominate two-photon absorption in GaAs (Ref. 22) and indeed in most semiconductors.[23–25] They are "allowed-forbidden" transitions because the intraband transition, proportional to the velocity of electrons in the band, is zero at the Γ point. Consequently, it is not possible to derive the two-photon degree of spin polarization using the states at the Γ point as can be done for one-photon excitation [Fig. 1(a)] or other two-photon transitions [Fig. 1(d)]. Instead, one must go away from the Γ point and sum over all $\mathbf{k}$ directions. With this caveat in mind, we nonetheless give a schematic illustration of a two-band transition in Fig. 1(c). One should bear in mind that, away from the Γ point, one cannot in general associate states in the heavy hole band with $J_z = \pm 3/2$ and states in the light hole band with $J_z = \pm 1/2$, since this is only true for $\mathbf{k} \| \mathbf{z}$. It is essentially due to this complication that the sum over directions of $\mathbf{k}$ gives a two-photon P that depends on the details of the bands.

The slower decrease of the two-photon P compared to the one-photon P at excess photon energies greater than the split-off energy can be understood from a consideration of two-band transitions. The one-photon P decreases in this regime due to the selection rules involving transitions from the split-off band.[1] The same selection rules apply to the interband part of the two-band transition, but the intraband part of transitions from the split-off band is much weaker than the transitions from the heavy and light hole bands, since the latter excite to states higher in the conduction band that have higher velocity.

There are also allowed-forbidden transitions of the three-band variety ($hh-lh-c$, $hh-so-c$, $lh-hh-c$, and $lh-so-c$); in these cases, the intervalence band matrix elements can connect states of opposite spin. Their effect on the two-photon spin polarization approximately cancels out in GaAs, as one can see by comparing a calculation that neglects them[17] with one that includes them.[16]

Within a spherical model, allowed-forbidden transitions must conserve angular momentum; two-photon absorption with circularly polarized light must transfer two units of angular momentum to each electron-hole pair that is created. In order to understand how this leads to an incomplete spin polarization, one should form eigenstates of angular momentum, even away from the Γ point. Such states can be formed in a spherical model with envelope functions over an expansion of Bloch states.[54] Any treatment of electron angular momentum must then take into account both the cell-periodic part and the envelope function part of the electron wave function. It is the latter that is neglected in the argument of Matsuyama.[14] We plan to return to a more detailed discussion of this issue in a future publication.

Yet even without that analysis it is clear that, in a simple two-band spherical model consisting of a single spin degenerate valence band and a single spin degenerate conduction band, the two units of angular momentum are divided equally between the two parts of the electron wave function. This can be inferred from the fact that the envelope function for the relative motion of the electron and hole has one unit of orbital angular momentum (i.e., it is a p wave).[27] A two-band spherical model can be mocked-up from an eight band spherical model by setting the heavy and light hole band masses equal.[24,51] Doing so with the formula for the two-photon P given by Bhat and Sipe,[17] one sees that in that case the two-photon P is 50% at the band edge. More generally, the maximum two-photon P in a spherical model is 64%.[16,17]

B. Allowed-allowed transitions

Allowed-allowed transitions are those for which both matrix elements in the two-photon amplitude (5) are nonzero at the Γ point. Allowed-allowed transitions have a different frequency dependence than allowed-forbidden transitions. Near $2\hbar\omega \gtrsim E_g$ the former varies as $(2\hbar\omega - E_g)^{1/2}$ while the latter as $(2\hbar\omega - E_g)^{3/2}$. Hence allowed-allowed transitions can dominate allowed-forbidden transitions in a frequency range close to the band edge. For GaAs, however, this range is only 10 meV.[21,22] As seen in the 14 band calculation shown in the inset of Fig. 2, the two-photon degree of spin polarization in this range can be very different from the rest of the spectrum. These transitions are necessarily due to lower symmetry parts of the Hamiltonian; in a system with true spherical symmetry one could not have a two-photon transition from a p state to an s state, since two-photon transitions cannot connect states of opposite parity.

The selection rules for allowed-allowed transitions are worked out in Appendix B. Consider first the simple approximation of vanishing interband spin-orbit coupling Δ^- (denoted $\bar{\Delta}$ in Ref. 31). Then the basis states given in Appendix A are the energy eigenstates at the Γ point. For σ^+ polarized light incident along [001], the only allowed-allowed transitions are depicted in Fig. 1(d); these can be derived from Table III of Lee and Fan.[24] The product of the two matrix elements in the two-photon amplitude is the same for both transitions. Thus if the spin-orbit splitting of the upper conduction bands Δ_0' can be neglected compared to the other energy differences, then P is zero [see Eq. (B7) with $\Delta^- = 0$]. For σ^+ polarized light incident along [111], the nonzero transitions are (i) $|\Gamma_{8v}', +1/2\rangle$ to $|\Gamma_{8c}', -3/2\rangle$ to $|\Gamma_{6c}', -1/2\rangle$; (ii) $|\Gamma_{8v}', +3/2\rangle$ to ($|\Gamma_{8c}', -1/2\rangle$ and $|\Gamma_{7c}', -1/2\rangle$) to $|\Gamma_{6c}', +1/2\rangle$; and (iii) $|\Gamma_{8v}', -3/2\rangle$ to ($|\Gamma_{8c}', -1/2\rangle$ and $|\Gamma_{7c}', -1/2\rangle$) to $|\Gamma_{6c}', +1/2\rangle$. Here the prime indicates that the states are rotated so that the quantization axis is [111] rather than [001]. If the spin-orbit splitting of the upper conduction bands Δ_0' can be neglected compared to the other energy differences, then the third of these is zero and the probability for the second is three times that of the first, resulting in $P = -0.5$ [see Eq. (B8)].

However, close to the band edge, where allowed-allowed transitions dominate, the full 14 band calculation (see Table II or the insets of Figs. 2–4) does not agree with these simple arguments. There is significant difference between materials; for GaAs $P = -0.21$ and $P = -0.60$ for light incident along [001] and [111], respectively. The disagreement is due to the importance of the spin-orbit mixing between the valence and upper conduction bands, characterized by a nonvanishing Δ^-.

The interband spin-orbit coupling Δ^- would be zero if the material had inversion symmetry.[33,55,56] In contrast to most of the other parameters in the 14 band model, the value of Δ^- has not been determined by directly fitting it to one or more experimental results. Rather, it has been calculated by vari-

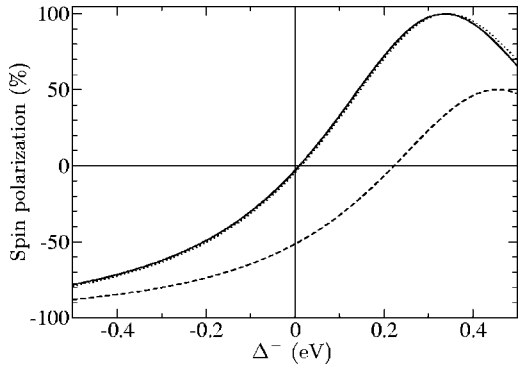

FIG. 7. Sensitivity of the GaAs band-edge two-photon P to Δ^-. The solid (dashed) line is for two-photon excitation with circularly polarized light incident along a $\langle 001\rangle$ ($\langle 111\rangle$) direction as calculated with the 14 band model. The dotted line is Eq. (B7).

ous methods: the empirical pseudopotential method (-61 meV for GaAs),[31,35,57] the tight binding method (-85 meV for GaAs),[33] the *ab initio* linear-muffin-tin-orbitals method (-110 meV for GaAs),[33] and by an indirect fitting with a 30×30 $\mathbf{k}\cdot\mathbf{p}$ Hamiltonian (-70 meV for GaAs).[33,56]

In light of the variation in calculated values of the interband spin-orbit coupling Δ^-, we have investigated the dependence of the band edge two-photon degree of spin polarization on Δ^-. The result, shown in Fig. 7, is rather dramatic. First, it shows that for small Δ^-, P due to [001] incident light is proportional to Δ^-, whereas P due to [111] incident light is less sensitive to Δ^-. Second, it indicates that a 100% degree of spin polarization could indeed be possible due to two-photon absorption. But this possibility is *not* due to the transfer of angular momentum from the light to the electrons. Since it results from allowed-allowed transitions that are only nonzero due to the lack of inversion symmetry and could only occur for certain crystal orientations, we suggest that some of the angular momentum comes from the crystal lattice itself.

The selection rules for allowed-allowed transitions including interband spin-orbit coupling are given for [001] incident light in Eqs. (B1)–(B6) and an expression for the resulting spin polarization is given in Eq. (B7). It is worth noting that P is independent of the valence-upper conduction momentum matrix parameter Q.

This allows us to see how the small spin-orbit mixing between valence and upper conduction bands can have an important effect on the band edge spin-polarization. Allowed-allowed transitions between the unmixed states [Fig. 1(d)] are proportional to the small matrix element P_0', which would be zero if there were inversion symmetry; and since the intermediate state is in an upper conduction band, the energy denominator of the two-photon transition amplitude is large, which further reduces the amplitude for these transitions. The interband spin-orbit mixing, proportional to Δ^-/E_0', is small, but it introduces allowed-allowed transitions with a valence band as an intermediate state. Then, instead of being proportional to P_0', the transition is proportional to P_0, and the energy denominator is smaller. This allows the condition $CP_0'=DP_0\Delta^-$ to be met with fairly modest interband spin-orbit mixing.

V. CONCLUSION

We have shown experimentally that the degrees of spin polarization produced by one- and two-photon spin injection are approximately equal in GaAs at an excess photon energy of 90 meV. This was also recently confirmed experimentally by Stevens *et al.*,[58] where for (111)-oriented GaAs the measured degree of spin polarization of electrons generated by one- and two-photon excitation was found to be the same, in accord with our measurements for (001)-oriented GaAs. The experimental results agree with our theoretical calculations, and they are not at odds with angular momentum conservation. As well, we have calculated the degree of spin polarization in other materials to show that the one- and two-photon degrees of spin polarization need not be equal.

We have presented the first calculation of two-photon spin injection that goes beyond a spherical model. The cubic anisotropy of the two-photon P is small for most of the semiconductors we investigated at photon energies where allowed-forbidden transitions dominate, although it is somewhat larger in ZnSe and InP than in the others. Allowed-allowed transitions, which do not appear in a spherical model, and hence do not conserve angular momentum, are found to strongly modify the two-photon P close to the band edge, and cause a large cubic anisotropy. We have identified the selection rules responsible for these transitions and found that interband spin-orbit coupling plays an important role.

Measuring the two-photon P due to allowed-allowed transitions would be challenging in most semiconductors, since they only dominate in a narrow energy range, and the absorption rate is small close to the band edge. However, such a measurement could serve as a means of determining the parameter Δ^-, which contributes to the electron g factor[33] and the spin splitting of bands.[31,37]

We emphasize that the calculations presented here are all in the independent particle approximation, and in particular neglect the Coulomb interaction between the optically excited electron and hole. Hence two-photon injection of spin-polarized bound excitons is outside the scope of this paper. Close to the band edge, excitonic effects are known to enhance two-photon absorption.[24,27,59–61] Two-photon spin injection will be similarly enhanced, and thus the two-photon P will be less sensitive to excitonic effects since it is a ratio of the two [see Eq. (10)]. Certainly, for excess photon energies greater than an exciton binding energy, we do not expect excitonic effects to greatly modify the results presented here. However, within an exciton binding energy of the band edge, the enhancements of allowed-allowed and allowed-forbidden transitions may differ,[60,61] envelope-hole coupling may modify the selection rules leading to two-photon spin injection,[62] and the electron spin lifetime will be shorter due to the Bir-Aronov-Pikus mechanism of spin relaxation.[63] Thus a complete theory of two-photon spin injection close to the band edge should include excitonic effects. Nonetheless, the two-photon P due to allowed-allowed transitions predicted here in the independent particle approximation should be observable in materials for which the dominance of allowed-allowed transitions extends beyond an exciton binding energy of the band edge.

ACKNOWLEDGMENTS

This work was financially supported by the Natural Science and Engineering Research Council, Photonics Research Ontario, the US Defense Advanced Research Projects Agency, and the US Office of Naval Research. The authors gratefully acknowledge many stimulating discussions with Wolfgang Rühle, Marty Stevens, Fred Nastos, Ali Najmaie, and Eugene Sherman.

APPENDIX A: NOTATION

The basis states for the 14 band model are (with $|\alpha_+\rangle = |\uparrow\rangle$ and $|\alpha_-\rangle = |\downarrow\rangle$),

$$|\Gamma_{7v}, \pm 1/2\rangle = \pm \frac{1}{\sqrt{3}}|Z\rangle|\alpha_\pm\rangle + \frac{1}{\sqrt{3}}|X \pm iY\rangle|\alpha_\mp\rangle;$$

$$|\Gamma_{8v}, \pm 1/2\rangle = \mp \sqrt{\frac{2}{3}}|Z\rangle|\alpha_\pm\rangle + \frac{1}{\sqrt{6}}|X \pm iY\rangle|\alpha_\mp\rangle;$$

$$|\Gamma_{8v}, \pm 3/2\rangle = \pm \frac{1}{\sqrt{2}}|X \pm iY\rangle|\alpha_\pm\rangle;$$

$$|\Gamma_{6v}, \pm 1/2\rangle = i|S\rangle|\alpha_\pm\rangle;$$

$$|\Gamma_{7c}, \pm 1/2\rangle = \pm \frac{1}{\sqrt{3}}|Z'\rangle|\alpha_\pm\rangle + \frac{1}{\sqrt{3}}|X' \pm iY'\rangle|\alpha_\mp\rangle;$$

$$|\Gamma_{8v}, \pm 1/2\rangle = \mp \sqrt{\frac{2}{3}}|Z'\rangle|\alpha_\pm\rangle + \frac{1}{\sqrt{6}}|X' \pm iY'\rangle|\alpha_\mp\rangle;$$

$$|\Gamma_{8v}, \pm 3/2\rangle = \pm \frac{1}{\sqrt{2}}|X' \pm iY'\rangle|\alpha_\mp\rangle,$$

where under the point group T_d, $|S\rangle$ transforms like Γ_1, while $\{|X\rangle, |Y\rangle, |Z\rangle\}$ and $\{|X'\rangle, |Y'\rangle, |Z'\rangle\}$ transform like Γ_4.[35]

At the Γ point, the energy between Γ_{6c} and Γ_{8v} bands is E_g, the energy between Γ_{7c} and Γ_{8v} bands is E_0', the energy between Γ_{8v} and Γ_{7v} bands is Δ_0, and the energy between Γ_{8c} and Γ_{7c} bands is Δ_0'. The momentum matrix elements are $P_0 = i(\hbar/m)\langle X|p^x|S\rangle$, $P_0' = i(\hbar/m)\langle X'|p^x|S\rangle$, and $Q = i(\hbar/m)\langle X'|p^y|Z\rangle$, where m is the electron mass. The interband spin-orbit coupling is

$$\Delta^- = \frac{3i\hbar}{4m^2c^2}\langle Z'|(\nabla V \times \mathbf{p})^y|X\rangle,$$

and its sign has been discussed by Cardona *et al.*[33] The parameters γ_{1L}, γ_{2L}, and γ_{3L} are the usual Luttinger parameters that account for remote band effects on the valence bands. Since the 14 band model accounts for the Γ_{6c}, Γ_{7c}, and Γ_{8c} bands exactly, modified Luttinger parameters are used in the 14×14 Hamiltonian.[31] The parameter F accounts for remote band effects on the conduction band (Γ_{6c}), essentially fixing its effective mass to the experimentally observed value. Finally, the parameter C_k is the small k-linear term in the valence bands due to interactions with remote bands.[33]

APPENDIX B: ALLOWED-ALLOWED CONTRIBUTION TO TWO-PHOTON SPIN INJECTION

To calculate $\dot{\mathbf{S}}$ and $\dot{\mathbf{N}}$ due to allowed-allowed transitions, we can approximate all the matrix elements and energies in the two-photon amplitude by their value at the Γ point, thus avoiding the integral over $\mathbf{k}$. Since the bands are doubly degenerate at the Γ point, we can use Eq. (4).

1. Light incident along [001]

Since we use a basis of states with spin quantized along $\hat{\mathbf{z}}$, $\langle c,\Gamma|\hat{S}^z|c',\Gamma\rangle \propto \delta_{c,c'}$ and we have

$$\dot{S}^z = \frac{\pi\hbar}{L^3}\sum_v \left[|\Omega^{(2)}_{c\uparrow,v,\Gamma}|^2 - |\Omega^{(2)}_{c\downarrow,v,\Gamma}|^2\right]\sum_k \delta[2\omega - \omega_{cv}(k)],$$

where $c\uparrow$ and $c\downarrow$ are shorthand for the bands with states $|\Gamma_{6c}, \pm 1/2\rangle$.

For σ^+ light, with polarization $\hat{\mathbf{e}}_\omega = (\hat{\mathbf{x}} + i\hat{\mathbf{y}})/\sqrt{2}$, and $\dot{\mathbf{S}} \| \hat{\mathbf{z}}$ from Eq. (2), the degree of spin polarization is

$$P = \frac{\sum_v \left[|\Omega^{(2)}_{c\downarrow,v,\Gamma}|^2 - |\Omega^{(2)}_{c\uparrow,v,\Gamma}|^2\right]}{\sum_v \left[|\Omega^{(2)}_{c\downarrow,v,\Gamma}|^2 + |\Omega^{(2)}_{c\uparrow,v,\Gamma}|^2\right]}.$$

All but the Γ_{6c} states are not eigenstates at the Γ point due to spin-orbit coupling between upper conduction and valence bands parameterized by Δ^-. The Hamiltonian at the Γ point in this basis has off-diagonal elements, but the order of the basis can be arranged so that it is block diagonal with blocks at most 2×2. For the bands $|\Gamma_{7v}, +1/2\rangle$ and $|\Gamma_{7c}, +1/2\rangle$ (or for the bands $|\Gamma_{7v}, -1/2\rangle$ and $|\Gamma_{7c}, -1/2\rangle$), the block is

$$\begin{bmatrix} -E_g - \Delta_0 & -2\Delta^-/3 \\ -2\Delta^-/3 & E_0' - E_g \end{bmatrix}.$$

Since $\Delta^-/(E_0' + \Delta_0) \ll 1$, the off-diagonal part can be treated perturbatively. To first order in the perturbation, we have eigenvectors

$$|so\uparrow/\downarrow\rangle = |\Gamma_{7v}, \pm 1/2\rangle + \frac{2\Delta^-}{3}\frac{1}{E_0' + \Delta_0}|\Gamma_{7c}, \pm 1/2\rangle;$$

$$|sc\uparrow/\downarrow\rangle = |\Gamma_{7c}, \pm 1/2\rangle - \frac{2\Delta^-}{3}\frac{1}{E_0' + \Delta_0}|\Gamma_{7v}, \pm 1/2\rangle.$$

For the Γ_8 bands, the blocks are

$$\begin{bmatrix} -E_g & \Delta^-/3 \\ \Delta^-/3 & E_0' - E_g + \Delta_0' \end{bmatrix}.$$

with eigenvectors to first order in $\Delta^-/(E_0' + \Delta_0')$,

$$|hh\uparrow/\downarrow\rangle = |\Gamma_{8v}, \pm 3/2\rangle - \frac{\Delta^-}{3}\frac{1}{E_0' + \Delta_0'}|\Gamma_{8c}, \pm 3/2\rangle;$$

$$|lh\uparrow/\downarrow\rangle = |\Gamma_{8v}, \pm 1/2\rangle - \frac{\Delta^-}{3}\frac{1}{E_0' + \Delta_0'}|\Gamma_{8c}, \pm 1/2\rangle;$$

$$|hc\uparrow/\downarrow\rangle = |\Gamma_{8c}, \pm 3/2\rangle + \frac{\Delta^-}{3}\frac{1}{E_0' + \Delta_0'}|\Gamma_{8v}, \pm 3/2\rangle;$$

$$|lc\uparrow/\downarrow\rangle = |\Gamma_{8c}, \pm 1/2\rangle + \frac{\Delta^-}{3}\frac{1}{E_0' + \Delta_0'}|\Gamma_{8v}, \pm 1/2\rangle.$$

The nonzero matrix elements of $\hat{\mathbf{e}}_\omega \cdot \hat{\mathbf{v}}$ in the eigenstate basis that can cause a two-photon transition between v and c are

$$\hbar \mathbf{e}_\omega \cdot \mathbf{v}_{hc\downarrow,lh\downarrow}(\Gamma) = -\sqrt{\frac{2}{3}}Q; \tag{B1}$$

$$\hbar \mathbf{e}_\omega \cdot \mathbf{v}_{c\downarrow,hc\downarrow}(\Gamma) = P_0' + \frac{\Delta^-}{3}\frac{1}{E_0' + \Delta_0'}P_0; \tag{B2}$$

$$\hbar \mathbf{e}_\omega \cdot \mathbf{v}_{sc\downarrow,lh\uparrow}(\Gamma) = -Q; \tag{B3}$$

$$\hbar \mathbf{e}_\omega \cdot \mathbf{v}_{c\uparrow,sc\downarrow}(\Gamma) = \sqrt{\frac{2}{3}}\left(P_0' - \frac{2\Delta^-}{3}\frac{P_0}{E_0' + \Delta_0}\right); \tag{B4}$$

$$\hbar \mathbf{e}_\omega \cdot \mathbf{v}_{so\downarrow,lh\uparrow}(\Gamma) = \frac{-\Delta^- Q/3}{E_0' + \Delta_0}\left(\frac{E_0' + \Delta_0}{E_0' + \Delta_0'} + 2\right); \tag{B5}$$

$$\hbar \mathbf{e}_\omega \cdot \mathbf{v}_{c\uparrow,so\downarrow}(\Gamma) = \sqrt{\frac{2}{3}}\left(P_0 + \frac{2\Delta^-}{3}\frac{P_0'}{E_0' + \Delta_0}\right), \tag{B6}$$

where we have dropped terms second order in Δ^-. Note that $\mathbf{e}_\omega \cdot \mathbf{v}_{hh\downarrow,lh\downarrow}(\Gamma) = 0$ by an exact cancellation, as it should from symmetry considerations. Thus we have

$$\Omega^{(2)}_{c\downarrow,lh\downarrow,\Gamma} = -\frac{e^2}{\hbar^3\omega^2}|E_\omega|^2\sqrt{\frac{2}{3}}Q[AP_0' + BP_0\Delta^-],$$

where $A \equiv (E_0' + \Delta_0' - E_g/2)^{-1}$ and $B \equiv (E_0' + \Delta_0')^{-1}A/3$. We also have

$$\Omega^{(2)}_{c\uparrow,lh\uparrow,\Gamma} = -\frac{e^2}{\hbar^3\omega^2}|E_\omega|^2\sqrt{\frac{2}{3}}Q[CP_0' - DP_0\Delta^-],$$

where $C \equiv (E_0' - E_g/2)^{-1}$,

$$D \equiv \frac{1}{E_0' + \Delta_0}\left[\frac{1}{E_g/2 + \Delta_0}\frac{1}{3}\left(\frac{E_0' + \Delta_0}{E_0' + \Delta_0'} + 2\right) + \frac{2}{3}C\right],$$

and we have dropped terms proportional to $QP_0'(\Delta^-)^2$. The degree of spin polarization is then

$$P = \frac{(AP_0' + BP_0\Delta^-)^2 - (CP_0' - DP_0\Delta^-)^2}{(AP_0' + BP_0\Delta^-)^2 + (CP_0' - DP_0\Delta^-)^2}. \tag{B7}$$

2. Light incident along [111]

For σ^+ light incident along [111], it is more tedious to obtain an expression like Eq. (B7) since there are more nonzero matrix elements of $\hat{\mathbf{e}}_\omega \cdot \hat{\mathbf{v}}$ than for σ^+ light incident along [001]. By rotating the basis to states quantized along [111], the matrix of elements of $\hat{\mathbf{e}}_\omega \cdot \hat{\mathbf{v}}$ becomes simpler, but the Hamiltonian is no longer in 2×2 blocks. When $\Delta^- = 0$, the latter is not an issue. In that case, we find

$$\Omega^{(2)}_{c\downarrow,lh\uparrow,\Gamma} = \frac{e^2}{\hbar^3\omega^2}|E_\omega|^2\frac{2}{3}iQP_0'A,$$

$$\Omega^{(2)}_{c\uparrow,hh\uparrow,\Gamma} = \frac{e^2}{\hbar^3\omega^2}|E_\omega|^2\frac{2}{3}iQP_0'\frac{1}{\sqrt{3}}(A + 2C),$$

$$\Omega^{(2)}_{c\uparrow,hh\downarrow,\Gamma} = -\frac{e^2}{\hbar^3\omega^2}|E_\omega|^2 iQP_0'\frac{1}{3}\sqrt{\frac{2}{3}}(C - A),$$

where A and C are as defined in the previous section, and $\uparrow$ and $\downarrow$ are along [111]. With the assumption that $\Delta_0' \ll E_0' - E_g/2$, $A \approx C$ and we find that

$$P(\Delta^- = 0) = -1/2. \tag{B8}$$

*Present address: Charles University in Prague, Faculty of Mathematics and Physics, Ke Karlovu 3, 121 16 Prague 2, Czech Republic.

[1] M. I. Dyakonov and V. I. Perel, in *Optical Orientation*, edited by F. Meier and B. Zakharchenya (North-Holland, Amsterdam, 1984), Vol. 8 of *Modern Problems in Condensed Matter Sciences*, Chap. 2.

[2] *Semiconductor Spintronics and Quantum Computation*, edited by D. D. Awschalom, D. Loss, N. Samarth (Springer, Berlin, 2002).

[3] I. Žutić, J. Fabian, and S. Das Sarma, Rev. Mod. Phys. **76**, 323 (2004).

[4] T. Maruyama, E. L. Garwin, R. Prepost, G. H. Zapalac, J. S. Smith, and J. D. Walker, Phys. Rev. Lett. **66**, 2376 (1991).

[5] T. Omori, Y. Kurihara, T. Nakanishi, H. Aoyagi, T. Baba, T. Furuya, K. Itoga, M. Mizuta, S. Nakamura, Y. Takeuchi, M. Tsubata, and M. Yoshioka, Phys. Rev. Lett. **67**, 3294 (1991).

[6] F. Ciccaci, E. Molinari, and N. E. Christensen, Solid State Commun. **62**, 1 (1987).

[7] S.-H. Wei and A. Zunger, Appl. Phys. Lett. **64**, 1676 (1994).

[8] A. Janotti and S.-H. Wei, Appl. Phys. Lett. **81**, 3957 (2002).

[9] E. L. Ivchenko, Sov. Phys. Solid State **14**, 2942 (1973).

[10] A. M. Danishevskii, Sov. Phys. Solid State **20**, 1818 (1978).

[11] A. M. Danishevskii, Sov. Phys. Solid State **29**, 575 (1987).

[12] M. S. Bresler, O. B. Gusev, and I. A. Merkulov, Sov. Phys. JETP **66**, 1179 (1987).

[13] M. S. Bresler, O. B. Gusev, and I. Merkulov, Sov. Phys. Solid

State **30**, 99 (1988).
[14] T. Matsuyama, H. Horinaka, W. Wada, T. Kondo, M. Hangyo, T. Nakanishi, S. Okumi, and K. Togawa, Jpn. J. Appl. Phys., Part 2 **40**, L555 (2001).
[15] A. M. Danishevskii, E. L. Ivchenko, S. F. Kochegarov, and M. I. Stepanova, JETP Lett. **16**, 440 (1972).
[16] S. B. Arifzhanov and E. L. Ivchenko, Sov. Phys. Solid State **17**, 46 (1975).
[17] R. D. R. Bhat and J. E. Sipe, Phys. Rev. Lett. **85**, 5432 (2000).
[18] P. Y. Yu and M. Cardona, *Fundamentals of Semiconductors* (Springer, Berlin, 1996), Chap. 2.
[19] E. O. Kane, J. Phys. Chem. Solids **1**, 249 (1957).
[20] M. D. Dvorak, W. A. Schroeder, D. R. Anderson, A. L. Smirl, and B. S. Wherrett, IEEE J. Quantum Electron. **30**, 256 (1994).
[21] D. C. Hutchings and B. S. Wherrett, Phys. Rev. B **49**, 2418 (1994).
[22] J. P. van der Ziel, Phys. Rev. B **16**, 2775 (1977).
[23] I. M. Catalano, A. Cingolani, and M. Lepore, Phys. Rev. B **33**, 7270 (1986).
[24] C. C. Lee and H. Y. Fan, Phys. Rev. B **9**, 3502 (1974).
[25] V. I. Bredikhin, M. D. Galanin, and V. N. Genkin, Sov. Phys. Usp. **16**, 299 (1973).
[26] A. Najmaie, R. D. R. Bhat, and J. E. Sipe, Phys. Rev. B **68**, 165348 (2003).
[27] G. D. Mahan, Phys. Rev. **170**, 825 (1968).
[28] D. J. Hilton and C. L. Tang, Phys. Rev. Lett. **89**, 146601 (2002).
[29] G. Dresselhaus, Phys. Rev. **100**, 580 (1955).
[30] G. E. Pikus, V. A. Marushchak, and A. N. Titkov, Sov. Phys. Semicond. **22**, 115 (1988).
[31] P. Pfeffer and W. Zawadzki, Phys. Rev. B **53**, 12 813 (1996).
[32] R. D. R. Bhat, F. Nastos, A. Najmaie, and J. E. Sipe, cond-mat/0404066.
[33] M. Cardona, N. E. Christensen, and G. Fasol, Phys. Rev. B **38**, 1806 (1988).
[34] U. Rössler, Solid State Commun. **49**, 943 (1984).
[35] P. Pfeffer and W. Zawadzki, Phys. Rev. B **41**, 1561 (1990).
[36] H. Mayer and U. Rössler, Phys. Rev. B **44**, 9048 (1991).
[37] H. Mayer and U. Rössler, Solid State Commun. **87**, 81 (1993).
[38] H. Mayer, U. Rössler, and M. Ruff, Phys. Rev. B **47**, 12 929 (1993).
[39] D. C. Hutchings and B. S. Wherrett, Phys. Rev. B **52**, 8150 (1995).
[40] D. C. Hutchings and J. M. Arnold, Phys. Rev. B **56**, 4056 (1997).
[41] R. Winkler, *Spin-Orbit Coupling Effects in Two-Dimensional Electron and Hole Systems*, Vol. 191 of *Springer Tracts in Modern Physics* (Springer, Berlin, 2003).
[42] P. Enders, A. Bärwolff, M. Woerner, and D. Suisky, Phys. Rev. B **51**, 16 695 (1995).
[43] T. E. Ostromek, Phys. Rev. B **54**, 14 467 (1996).
[44] A. Baldereschi and N. O. Lipari, Phys. Rev. B **8**, 2697 (1973).
[45] Y. Kerachian *et al.* (unpublished).
[46] M. K. Reed and M. K. S. Shepard, IEEE J. Quantum Electron. **32**, 1273 (1996).
[47] *Handbook of Optical Constants of Solids*, edited by E. D. Palik (Academic Press, Orlando, 1985), p. 439.
[48] M. I. DYakanov and V. I. Perel, Sov. Phys. JETP **33**, 1053 (1971).
[49] J. M. Kikkawa and D. D. Awschalom, Phys. Rev. Lett. **80**, 4313 (1998).
[50] P. H. Song and K. W. Kim, Phys. Rev. B **66**, 035207 (2002).
[51] A. Baldereschi and N. O. Lipari, Phys. Rev. Lett. **25**, 373 (1970).
[52] A. Baldereschi and N. O. Lipari, Phys. Rev. B **3**, 439 (1971).
[53] N. O. Lipari and A. Baldereschi, Phys. Rev. Lett. **25**, 1660 (1970).
[54] K. J. Vahala and P. C. Sercel, Phys. Rev. Lett. **65**, 239 (1990).
[55] M. Cardona, F. H. Pollak, and J. Broerman, Phys. Lett. **19**, 276 (1965).
[56] F. H. Pollak, C. W. Higginbotham, and M. Cardona, J. Phys. Soc. Jpn. **21**, 20 (1966).
[57] I. Gorczyca, P. Pfeffer, and W. Zawadzki, Semicond. Sci. Technol. **6**, 963 (1991).
[58] M. J. Stevens, R. D. R. Bhat, J. E. Sipe, H. M. van Driel, and A. L. Smirl, Phys. Status Solidi B **238**, 568 (2003).
[59] R. Loudon, Proc. Phys. Soc. London **80**, 952 (1962).
[60] K. C. Rustagi, F. Pradere, and A. Mysyrowicz, Phys. Rev. B **8**, 2721 (1973).
[61] E. Doni, G. P. Parravicini, and R. Girlanda, Solid State Commun. **14**, 873 (1974).
[62] M. Sondergeld, Phys. Status Solidi B **81**, 451 (1977).
[63] G. L. Bir, A. G. Aronov, and G. E. Pikus, Sov. Phys. JETP **42**, 705 (1976).